Bull. Chem. Soc. Jpn., 70, 3031—3040 (1997)

Structures and Magnetic Properties of Dinuclear Vanadium(III) Complexes with Alkoxo Bridge

Kan Kanamori*, Kaori Yamamoto, Takako Okayasu, Naoto Matsui, Ken-ichi Okamoto,† and Wasuke Mori††

Department of Chemistry, Faculty of Science, Toyama University, Gofuku 3190, Toyama 930

†Department of Chemistry, University of Tsukuba, Tsukuba, Ibaraki 305

††Department of Material Science, Kanagawa University, Tsuchiya 2946, Hiratsuka, Kanagawa 259-12

(Received July 14, 1997)

Several dinuclear vanadium(III) complexes were prepared using a heptadentate dinucleating ligand containing a bridging alkoxo group. The structures of $[V_2(dpot)(m\text{-hbza})(H_2O)_2]\cdot H_2O$ (**1b**), $[V_2(bza)(OH)(tphpn)(H_2O)_2]Cl_3\cdot 8H_2O$ (**2**), and $[V_2(hpnbpda)_2]\cdot 12H_2O$ (**3a**) were determined by X-ray crystallography (dpot: 2-oxo-1,3-diaminopropane-*N*,*N*,*N*′,*N*′-tetraacetate, *m*-hbza: *m*-hydroxybenzoate, bza: benzoate, tphpn: *N*,*N*,*N*′,*N*′-tetrakis(2-pyridylmethyl)-2-oxo-1,3-propanediamine, hpnbpda: *N*,*N*′-bis(2-pyridylmethyl)-2-oxo-1,3-propanediamine-*N*,*N*′-diacetate). Each vanadium(III) center of **1b** adopts a distorted octahedral structure, and the two vanadium centers are bridged by an alkoxo group of dpot and a carboxylato group of *m*-hbza bridge. Each vanadium center of **2** and **3a**, however, takes a heptacoordinate structure. The coordination polyhedron of **2** can be regarded as a capped octahedron, while that of **3a** as a pentagonal bipyramid. The two vanadium(III) centers are ferromagnetically coupled in **1b** ($J = 23.7\ cm^{-1}$) and **2** ($J = 14.6\ cm^{-1}$), whereas in **3a** they are antiferromagnetically coupled ($J = -35.2\ cm^{-1}$). The electrochemistry of the dpot and hpnbpda complexes has also been investigated.

The structures of dinuclear vanadium(III) complexes with a heptadentate dinucleating ligand containing a bridging alkoxo group have been studied. It has been shown that 2-oxo-1,3-diaminopropane-*N*,*N*,*N*′,*N*′-tetraacetate (dpot) yields a 2:2 dinuclear vanadium(III) complex, $[V_2(Hdpot)_2]^{2-}$, where the two vanadium(III) atoms are bridged by two alkoxo groups and each vanadium center adopts a heptacoordinate structure.[1] We have reported the preliminary result that dpot also yields a 2:1 dinuclear vanadium(III) complex doubly bridged by an alkoxo group of dpot and a carboxylato group of benzoate (bza) or hydroxybenzoate (hbza), $[V_2(dpot)(bza\text{ or }hbza)(H_2O)_2]$.[2] Each vanadium(III) atom takes a hexacoordinate structure in the 2:1 dinuclear complex.

We have also shown in the preliminary report that a tphpn ligand, where tphpn denotes *N*,*N*,*N*′,*N*′-tetrakis(2-pyridylmethyl)-2-oxo-1,3-diaminopropane, behaves differently from dpot in constructing dinuclear vanadium(III) complexes.[3] Namely, a 2:2 complex corresponding to $[V_2(Hdpot)_2]^{2-}$ was not obtained with this ligand. Furthermore, the dinuclear vanadium(III) complex obtained using tphpn and benzoate as bridging ligands has been revealed to be a triply bridged complex with an additional hydroxo bridge, $[V_2(bza)(OH)(tphpn)(H_2O)_2]Cl_3$. The vanadium(III) center adopts a heptacoordination in this complex.

A hpnbpda ligand has an intermediate structure between dpot and tphpn (see Scheme 1), where hpnbpda denotes *N*,*N*′-bis(2-pyridylmethyl)-2-oxo-1,3-diaminopropane-*N*,*N*′-diacetate. It is, therefore, of interest to examine what type of dinuclear vanadium(III) complex hpnbpda would give.

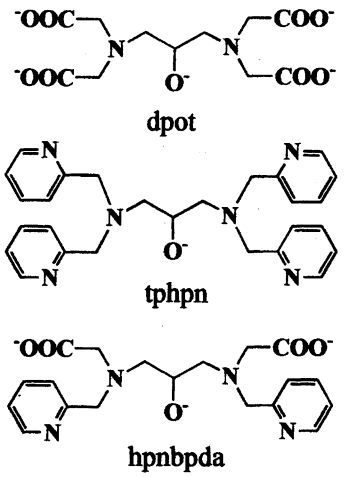

Scheme 1.

In addition to the diverse coordination stereochemistry of dinuclear vanadium(III) complexes, the magnetic exchange interactions between two vanadium(III) centers also significantly change depending on the bridging modes. Dinuclear vanadium(III) complexes having a single oxo bridge exhibit very strong ferromagnetic interactions with $J > +200\ cm^{-1}$.[4—6] Although dinuclear vanadium(III) complexes triply bridged by one oxo and two carboxylato

groups also exhibit ferromagnetic interactions with J values in the range of 20—30 cm^{-1}, they switch to antiferromagnetic interactions upon protonation of the oxo bridge.[7—9] On the other hand, dinuclear vanadium(III) complexes having two alkoxo or phenoxo bridges show antiferromagnetic interactions.[1b,10,11] Dinuclear vanadium(III) complexes with halogeno bridges also exhibit antiferromagnetic interactions.[12—14] The dinuclear vanadium(III) complex, which contains an oxo and two sulfito bridges, and a direct V–V bond shows a very strong antiferromagnetic interaction with J of -355 cm^{-1}.[15] It is, therefore, of importance to clarify magnetic-exchange interactions in several types of dinuclear vanadium(III) complexes obtained here. We herein report on the structures and magnetic properties of dinuclear vanadium(III) complexes containing several alkoxo-bridging dinucleating ligands. The electrochemical properties of $[V_2(dpot)(bza)(H_2O)_2]$ and $[V_2(hpnbpda)_2]$ are also presented.

Experimental

Preparation of Ligands. 2-Hydroxy-1,3-diaminopropane-*N,N,N′,N′*-tetraacetic Acid (H_5dpot). H_5dpot was obtained commercially and used as received.

***N,N,N′,N′*-Tetrakis(2-pyridylmethyl)-2-hydroxy-1,3-propanediamine (Htphpn·4$HClO_4$).** Htphpn has already been prepared, as mentioned in the literature,[16,17] though the detailed procedure has not been described. We prepared Htphpn by the following method. Solid sodium hydroxide (6.4 g, 0.16 mol) was slowly added to an aqueous solution (100 cm^3) containing 1,3-diamino-2-hydroxypropane (1.8 g, 0.02 mol) and 2-picolyl chloride hydrochloride (13.1 g, 0.08 mol), while the mixture was cooled in an ice bath. Stirring was continued at room temperature for one day; then, a red oil was separated. The red oil was extracted with chloroform and the organic extract was washed with cold water three times. Evaporation of the solvent under reduced pressure afforded a red oily product, which was dissolved in 200 cm^3 of ethanol. Excess perchloric acid (60%) was added to the ethanol solution with stirring, resulting in the precipitation of a brown powder. The brown powder was collected by filtration, washed with ethanol, and recrystallized from hot water. Yield, 12 g (71%). Found: C, 37.77; H, 3.91; N, 9.81%. Calcd for $C_{27}H_{30}N_6O$·4$HClO_4$: C, 37.86; H, 4.00; N, 9.82%.

2-Hydroxy-1,3-diaminopropane-*N,N′*-diacetic Acid (H_3hpnda). To an aqueous solution (200 cm^3) of glycine (37.5 g, 0.5 mol) neutralized with lithium hydroxide (21 g, 0.5 mol) was added 1,3-dichloro-2-propanol (32.3 g, 0.25 mol). Solid lithium hydroxide (21 g, 0.5 mol) was added in small portions to the solution with stirring while the mixture was cooled in an ice bath. Stirring was continued at 40 °C for 3 d. The pH of the solution was adjusted to 5 by adding hydrobromic acid. The solution was concentrated under vacuum until precipitation began; the mixture was kept standing at room temperature to complete precipitation. A white precipitate was collected by filtration, washed with ethanol and ether, and dried in air. Yield, 32 g (33%). Found: C, 22.39; H, 4.58; N, 7.23%. Calcd for $C_7H_{14}N_2O_5$·2HBr·0.5H_2O: C, 22.30; H, 4.55; N, 7.43%.

***N,N′*-Bis(2-pyridylmethyl)-2-hydroxy-1,3-propanediamine-*N,N′*-diacetic Acid (H_3hpnbpda).** Solid 2-picolyl chloride hydrochloride (16.4 g, 0.1 mol) was added to an aqueous solution (100 cm^3) of H_3hpnda·2HBr·0.5H_2O (18.9 g, 0.05 mol) neutralized with lithium hydroxide (8.4 g, 0.2 mol). Solid lithium hydroxide (8.4 g, 0.2 mol) was added in small portions with vigorous stirring while the mixture was cooled in an ice bath. Stirring was continued at room temperature for one day, resulting in a homogeneous dark-red solution. The pH of the solution was adjusted to 5 by adding hydrobromic acid. After the solution was concentrated to ca. 50 cm^3 under vacuum, 50 cm^3 of ethanol was added. An off-white powder was precipitated by adding acetone. The product was collected by filtration, washed with acetone, and recrystallized from a small amount of water by adding ethanol and acetone. Yield, 19.5 g (75%). Found: C, 43.79; H, 5.69; N, 10.85%. Calcd for $C_{19}H_{24}N_4O_5$·HBr·3H_2O: C, 43.59; H, 5.98; N, 10.71%.

Preparation of Complexes. All manipulation was carried out under an argon atmosphere using standard Schlenk techniques or in a nitrogen-filled dry box. The preparative methods of $[V_2(dpot)(bza$ or *m*-hbza$)(H_2O)_2]$·H_2O (**1a** or **1b**) as well as *o*- and *p*-hbza analogues have been described in our preliminary reports.[2] (ν_{as}(COO): 1667, 1628 cm^{-1} (IR) 1601 cm^{-1} (Raman), ν_s(COO): 1418 cm^{-1} (IR), 1418 cm^{-1} (Raman) for the bza complex; ν_{as}(COO): 1669, 1629 cm^{-1} (IR), 1614 cm^{-1} (Raman), ν_s(COO): 1382 cm^{-1} (IR), 1386 cm^{-1} (Raman) for the *o*-hbza complex; ν_{as}(COO): 1672, 1633 cm^{-1} (IR), 1624 cm^{-1} (Raman), ν_s(COO): 1413 cm^{-1} (IR), 1415 cm^{-1} (Raman) for the *m*-hbza complex; ν_{as}(COO): 1672, 1617 cm^{-1} (IR), 1598 cm^{-1} (Raman), ν_s(COO): 1416 cm^{-1} (IR) 1412 cm^{-1} (Raman) for the *p*-hbza complex.) The synthesis of $[V_2(bza)(OH)(tphpn)(H_2O)_2]Cl_3$·8$H_2O$ (**2**) have also been described earlier.[3] (ν_{as}(COO): 1546 cm^{-1} (IR), ν_s(COO): 1412 cm^{-1} (IR).)

$[V_2(hpnbpda)_2]$·12H_2O (Orange Form, 3a) and $[V_2(hpnbpda)_2]$·7.5H_2O (Yellow Form, 3b). An aqueous solution (20 cm^3) containing 2.1 g (4 mmol) of H_3hpnbpda·HBr·3H_2O and 0.67 g (16 mmol) of LiOH was mixed with a solution (10 cm^3) of VCl_3 (0.63 g, 4 mmol). Allowing the resulting brown solution to stand at room temperature afforded orange and yellow crystals. Yield, 0.2 g (9%) for **3a** and 0.4 g (20%) for **3b**. Found for **3a**: C, 42.02; H, 5.90; N, 10.31%. Calcd for $C_{38}H_{42}N_8O_{10}V_2$·12H_2O: C, 41.91; H, 6.12; N, 10.29%. Found for **3b**: C, 45.26; H, 5.57; N, 11.12%. Calcd for $C_{38}H_{42}H_8O_{10}V_2$·7.5H_2O: C, 45.28; H, 5.71; N, 11.12%. IR for **3a**: 1645 cm^{-1} (ν_{as}(COO)), 1379 cm^{-1} (ν_s(COO)). IR for **3b**: 1640 cm^{-1} (ν_{as}(COO)), 1378 cm^{-1} (ν_s(COO)).

$[V_2(hpnbpda)(bza)(H_2O)_2]Cl_2$·4$H_2O$ (4). H_3hpnbpda·HBr·3H_2O (0.21 g, 0.4 mmol) in water (20 cm^3) was neutralized with lithium hydroxide (0.07 g, 1.6 mmol). This solution was mixed with an aqueous solution (10 cm^3) of VCl_3 (0.13 g, 0.8 mmol), then benzoic acid (0.05 g, 0.4 mmol) in 5 cm^3 of methanol was added. Allowing the resulting brown solution of stand at 50 °C afforded small green crystals. This complex is fairly sensitive to air-oxidation. Yield, 0.23 g (77%). Found: C, 41.75; H, 4.48; N, 7.44%. Calcd for $C_{26}H_{26}N_4O_7Cl_2V_2$·4$H_2O$: C, 41.56; H, 4.57; N, 7.46%. IR: 1653, 1542 cm^{-1} (ν_{as}(COO)), 1404 cm^{-1} (ν_s(COO)). UV-vis (DMSO) λ/nm (ε/mol^{-1} dm^3 cm^{-1}): 600 (70), 378 (684).

Measurements. UV-vis spectra were measured using a JASCO Ubest 50 spectrophotometer. Diffuse reflectance spectra were obtained for complexes diluted with MgO. The magnetic susceptibility was measured by the SQUID method using a Quantum Design MPMS-5S. Electrochemical experiments were carried out with a CV-27 apparatus [Biochemical Systems, Inc. (BAS)] using a glassy carbon working electrode. Ag/AgCl and platinum wire electrodes were used as reference and auxiliary electrodes, respectively. The electrochemistry of **1a** was investigated at room temperature in dimethylsulfoxide containing 0.1 mol dm^{-3} of $(n\text{-}Bu)_4NClO_4$ as the supporting electrolyte and 2 mmol dm^{-3} of the complex. Electro-

chemical experiments for **3a** and **3b** were conducted at room temperature in methanol containing 0.1 mol dm^{-3} of $(n\text{-Bu})_4NClO_4$ as the supporting electrolyte and 2 mmol dm^{-3} of **3a** or **3b**.

X-Ray Structure Determination. The crystallographic data are summarized in Table 1. Crystals were mounted on a glass fiber, coated with epoxy as a precaution against solvent loss, and centered on an Enraf–Nonius CAD4 (**1b** and **2**) or a Rigaku AFC7S (**3a**) diffractometer using graphite-monochromated Mo $K\alpha$ radiation. The unit-cell parameters were determined by a least-squares refinement, using the setting angles of 25 reflections in the range $16 < 2\theta < 20°$ for **1b**, $24 < 2\theta < 42°$ for **2**, and $14.8 < 2\theta < 15.0°$ for **3a**. Data reduction and the application of Lorentz, polarization, linear decay correction, and empirical absorption corrections based on a series of psi scans were carried out using the Enraf–Nonius Structure Determination Package[18] for **1b** and **2**, and AFC7S software (RIGAKU) for **3a**.

The structure was solved by a direct method (Ref. 18 or SIR92 in TEXSAN) and conventional difference Fourier techniques. The structures were refined by full-matrix least-squares techniques on F. All non-hydrogen atoms were refined anisotropically. The calculations were done on a VAX computer using the crystallographic package MOLEN[19] for **1b** and **2**, and on INDIGO II computer using the crystallographic package TEXSAN[20] for **3a**. A list of the full bond lengths and bond angles, anisotropic thermal parameters, hydrogen–atom positions, and $F_o - F_c$ tables were deposited as Document No. 70048 at the Office of the Editor of Bull. Chem. Soc. Jpn.

Results and Discussion

dpot Complex. Dinuclear vanadium(III) complexes, $[V_2(dpot)(bza \text{ or } hbza)(H_2O)_2]\cdot H_2O$, were obtained using benzoate or *o*-, *m*-, and *p*-hydroxybenzoate as a second bridging group in addition to a dinucleating dpot ligand. Since all of the complexes exhibit IR, Raman, and electronic spectral characteristics that are very similar to each other, the structures of these complexes must be basically the same. Since crystals of the best quality were obtained when *m*-hbza was used, the *m*-hbza complex was subjected to an X-ray structure analysis.

The final atomic coordinates and selected bond lengths and angles of $[V_2(dpot)(m\text{-hbza})(H_2O)_2]\cdot H_2O$ (**1b**) are listed in Tables 2 and 3, respectively. Figure 1 displays a perspective view of **1b** with its numbering scheme. **1b** is a dinuclear vanadium(III) complex doubly bridged by a deprotonated alkoxo group of dpot and a carboxylato group of *m*-hbza. The hydroxyl group of *m*-hbza is disordered in the crystal; O23, 30% and O24, 70%. Though the two vanadium(III) centers are unequivalent due to the coordination of an unsymmetrical *m*-hbza ligand, the geometry and dimensions around them are almost the same. Each vanadium(III) center adopts a hexacoordination, which is distinct from the heptacoordination in $[V_2(Hdpot)_2]^{2-}$,[1] and sits in a fairly distorted octahedron. The meridional coordination of the $N(CH_2COO^-)_2$ moiety of the dpot is responsible for this large distortion. Namely, two trans angles, O3–V1–O1 and O5–V2–O7, are 151.1(1)° and 151.6(1)°, respectively, which significantly deviate from the trans angle of a regular octahedron, 180°. In contrast to the above trans angles, the other trans angles are near to 180° (see Table 3).

The coordination bond lengths of dpot in **1b** are shorter

Table 1. Crystallographic Data

	$[V_2(dpot)(m\text{-hbza})(H_2O)_2]\cdot H_2O$	$[V_2(bza)(OH)(tphpn)(H_2O)_2]Cl_3\cdot 8H_2O$	$[V_2(hpnbpda)_2]\cdot 12H_2O$
Formula	$C_{18}H_{24}N_2O_{15}V_2$	$C_{34}H_{55}N_6O_{14}Cl_3V_2$	$C_{38}H_{66}N_8O_{22}V_2$
Formula wt	610.28	980.09	1088.86
Crystal system	Triclinic	Orthorhombic	Monoclinic
Space group	*P*1 (No. 2)	*Pbcm* (No. 57)	*C*2/*c* (No. 15)
a/Å	6.770(2)	10.546(1)	17.212(4)
b/Å	10.268(2)	18.898(1)	15.398(3)
c/Å	16.191(4)	22.333(1)	18.830(3)
α/°	83.31(2)		
β/°	84.57(2)		91.71(2)
γ/°	80.27(2)		
Z	2	4	4
V/Å^3	1098.5(4)	4451.0(6)	4988(1)
D_{calcd}/g cm^{-3}	1.84	1.45	1.45
Crystal size/mm	$0.10 \times 0.25 \times 0.50$	$0.13 \times 0.38 \times 0.45$	$0.38 \times 0.38 \times 0.50$
λ (Mo $K\alpha$)/Å	0.71073	0.71073	0.71069
μ (Mo $K\alpha$)/cm^{-1}	9.1	6.5	4.6
Scan width/°	0.8+0.35tan θ	0.5+0.49tan θ	1.15+0.30tan θ
Temp/K	296	296	296
2θ range/°	0—50	0—60	0—55
Reflctions			
Total	4013	7164	5925
$F_o > 3\sigma(F_o)$	3781	3528	3908
F(000)	624	2040	2288
No. of variables	394	298	325
R[a] (R_w)[b]	0.044 (0.050)	0.077 (0.079)	0.056 (0.068)

a) $R = (\sum(||F_o| - |F_c||)/\sum(|F_o|)$, b) $R_w = (\sum w(|F_o| - |F_c|)^2/\sum w(|F_o|^2)^{1/2}$.

Table 2. Final Atomic Coordinates and Equivalent Isotropic Thermal Parameters (B_{eq}/Å^2) for $[V_2(dpot)(m\text{-hbza})(H_2O)_2]\cdot H_2O$ ($B_{eq} = (8\pi^2/3)\sum\sum U_{ij} a_i^* a_j^* \boldsymbol{a}_i \cdot \boldsymbol{a}_j$)

Atom	x	y	z	B_{eq}
V1	0.81188(9)	0.43970(6)	0.81760(3)	1.55(1)
V2	0.92084(9)	0.17231(6)	0.68718(3)	1.65(1)
O1	0.5597(4)	0.4265(3)	0.8870(2)	2.33(5)
O2	0.2576(4)	0.5299(3)	0.9294(2)	3.28(7)
O3	1.0029(4)	0.5447(3)	0.7558(2)	2.14(5)
O4	1.0536(5)	0.7395(3)	0.6910(2)	3.06(6)
O5	1.1239(4)	0.2516(3)	0.6156(2)	2.18(5)
O6	1.2132(5)	0.3512(4)	0.4920(2)	4.62(8)
O7	0.7055(4)	0.0635(3)	0.7059(2)	2.66(6)
O8	0.4745(5)	−0.0220(3)	0.6505(3)	4.65(8)
O9	0.7759(4)	0.3413(2)	0.7239(1)	1.85(5)
O10	0.8579(4)	0.5535(3)	0.9111(2)	2.30(5)
O11	1.0811(4)	−0.0024(2)	0.6417(2)	2.18(5)
O21	0.9973(5)	0.2905(3)	0.8701(2)	2.79(6)
O22	1.0557(5)	0.1201(3)	0.7921(2)	3.04(6)
O23	1.2567(8)	0.1065(4)	1.1424(2)	3.8(1)
O24	1.403(2)	−0.241(1)	0.9795(7)	5.2(3)
N1	0.6070(4)	0.5947(3)	0.7562(2)	1.77(6)
N2	0.7568(5)	0.2351(3)	0.5777(2)	1.98(6)
C1	0.4139(6)	0.5230(4)	0.8836(2)	2.27(7)
C2	0.4460(6)	0.6401(4)	0.8198(2)	2.44(8)
C3	0.9409(6)	0.6619(4)	0.7209(2)	2.08(7)
C4	0.7194(6)	0.7005(4)	0.7177(2)	2.53(8)
C5	1.0934(6)	0.2984(4)	0.5386(2)	2.56(8)
C6	0.8986(7)	0.2786(5)	0.5084(2)	3.07(9)
C7	0.6015(6)	0.0486(4)	0.6457(3)	2.97(9)
C8	0.6588(6)	0.1239(4)	0.5621(3)	2.97(8)
C9	0.5217(6)	0.5292(4)	0.6933(2)	2.35(7)
C10	0.6841(6)	0.4297(4)	0.6565(2)	2.26(7)
C11	0.6005(6)	0.3461(4)	0.6023(2)	2.41(8)
C21	1.1674(7)	0.0853(4)	0.9283(2)	3.20(9)
C22	1.1733(8)	0.1377(4)	1.0038(3)	3.6(1)
C23	1.2531(8)	0.0544(5)	1.0707(3)	3.8(1)
C24	1.3260(8)	−0.0767(5)	1.0629(3)	3.8(1)
C25	1.3208(8)	−0.1285(5)	0.9875(3)	3.9(1)
C26	1.2413(8)	−0.0467(5)	0.9201(3)	3.7(1)
C27	1.0678(7)	0.1725(4)	0.8590(2)	2.77(8)

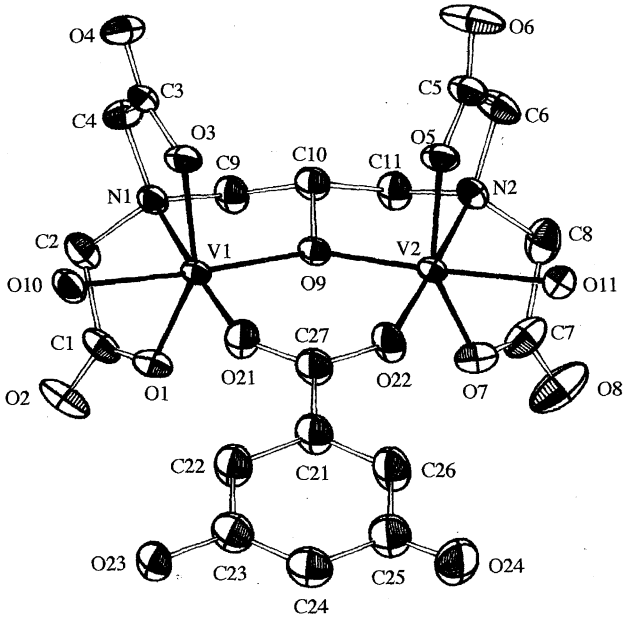

Fig. 1. Perspective view of $[V_2(dpot)(m\text{-hbza})(H_2O)_2]$ in **1b**.

Table 3. Selected Bond Distances (Å) and Angles (°) for $[V_2(dpot)(m\text{-hbza})(H_2O)_2]\cdot H_2O$

	Bond distances		
V1–O1	1.972(3)	V2–O7	1.966(3)
V1–O3	1.956(3)	V2–O5	1.941(3)
V1–O9	1.975(3)	V2–O9	1.971(2)
V1–O10	2.094(3)	V2–O11	2.108(2)
V1–O21	1.976(3)	V2–O22	1.983(3)
V1–N1	2.145(3)	V2–N2	2.160(3)
V1···V2	3.593(2)		
	Bond angles		
O1–V1–O3	151.1(1)	O5–V2–O7	151.6(1)
O1–V1–O9	101.0(1)	O7–V2–O9	100.3(1)
O1–V1–O10	81.9(1)	O7–V2–O11	81.7(1)
O1–V1–O21	101.7(1)	O7–V2–O22	100.5(1)
O1–V1–N1	78.4(1)	O7–V2–N2	78.0(1)
O3–V1–O9	95.8(1)	O5–V2–O9	95.3(1)
O3–V1–O10	80.6(1)	O5–V2–O11	81.9(1)
O3–V1–O21	100.7(1)	O5–V2–O22	101.9(1)
O3–V1–N1	80.3(1)	O5–V2–N2	80.6(1)
O9–V1–O10	176.2(1)	O9–V2–O11	176.8(1)
O9–V1–O21	93.4(1)	O9–V2–O22	93.9(1)
O9–V1–N1	83.6(1)	O9–V2–N2	83.0(1)
O10–V1–O21	88.5(1)	O11–V2–O22	88.2(1)
O10–V1–N1	94.5(1)	O11–V2–N2	95.0(1)
O21–V1–N1	177.0(1)	O22–V2–N2	176.2(1)
V1–O9–V2	131.3(1)		

on the average than those found in $[V_2(Hdpot)_2]^{2-}$, reflecting the smaller coordination number of **1b** than that of $[V_2(Hdpot)_2]^{2-}$.[1] On the contrary, the V···V distance (3.593(2) Å) is longer than the corresponding one (3.343 Å) in $[V_2(Hdpot)_2]^{2-}$ as a consequence of a larger alkoxo bridging angle (131.3(1)°), which is caused by the carboxylato bridge of *m*-hbza in **1b**, compared to that in $[V_2(Hdpot)_2]^{2-}$ (110.3°).

Since vanadium(III) complexes are substitution labile, the molecular structure found in the solid state is not always maintained in solution. We, therefore, compared the diffuse reflectance spectra with the absorption spectra of the solution to examine the structure of **1a** and **1b** in solution. The diffuse reflectance spectra of **1a** and **1b** show bands at 608 and 410 (shoulder) nm in the visible region. **1a** and **1b** are sparingly soluble in water, but are slightly soluble in dimethylsulfoxide. The absorption spectra in dimethylsulfoxide exhibit bands at the same positions as observed for the solid sample, indicating that the molecular structure found in the solid state is maintained in a dimethylsulfoxide solution.

tphpn Complex. It has been shown that a dinucleating ligand, tphpn, yields tetranuclear manganese complexes together with several kinds of additional bridging ligand.[21—24] Other transition-metal complexes containing tphpn have been scarcely found.

Although attempts to prepare a 2 : 2 vanadium(III)–tphpn

Table 4. Final Atomic Coordinates and Equivalent Isotropic Thermal Parameters (B_{eq}/Å^2) for $[V_2(bza)(OH)(tphpn)(H_2O)_2]Cl_3 \cdot 8H_2O$ ($B_{eq}=(8\pi^2/3)\sum\sum U_{ij}a_i^* a_j^* \boldsymbol{a}_i \cdot \boldsymbol{a}_j$)

Atom	x	y	z	B_{eq}
V	0.51709(8)	0.76856(5)	0.32227(4)	2.52(1)
O1	0.6125(5)	0.7322(3)	0.250	2.9(1)
O2	0.4617(5)	0.8252(3)	0.250	2.9(1)
O1d	0.3773(4)	0.6977(2)	0.3004(2)	3.20(8)
O1w	0.3660(4)	0.8214(2)	0.3649(2)	3.52(9)
N1	0.7090(4)	0.7364(3)	0.3556(2)	2.88(9)
N1a	0.4964(5)	0.6976(3)	0.4037(2)	3.13(9)
N1b	0.6187(5)	0.8641(2)	0.3503(2)	2.98(9)
C1	0.8030(5)	0.7448(3)	0.3063(3)	3.2(1)
C2	0.7427(7)	0.7127(4)	0.250	2.7(1)
C1a	0.5926(6)	0.6536(3)	0.4158(3)	3.2(1)
C2a	0.5883(7)	0.6025(3)	0.4614(3)	3.9(1)
C3a	0.4783(7)	0.5970(4)	0.4956(3)	4.4(1)
C4a	0.3760(7)	0.6413(4)	0.4839(3)	4.3(1)
C5a	0.3884(7)	0.6914(4)	0.4368(3)	4.0(1)
C6a	0.7057(6)	0.6611(3)	0.3760(3)	3.3(1)
C1b	0.7154(6)	0.8573(3)	0.3896(3)	3.3(1)
C2b	0.7799(7)	0.9158(4)	0.4126(3)	4.2(1)
C3b	0.7431(7)	0.9833(4)	0.3946(3)	4.5(2)
C4b	0.6444(7)	0.9908(4)	0.3542(3)	4.4(2)
C5b	0.5849(6)	0.9303(3)	0.3324(3)	3.5(1)
C6b	0.7457(6)	0.7827(3)	0.4069(3)	3.6(1)
C1d	0.2079(8)	0.6428(4)	0.250	2.7(1)
C2d	0.1516(6)	0.6245(3)	0.3047(3)	3.5(1)
C3d	0.0369(7)	0.5867(4)	0.3047(3)	4.7(2)
C4d	−0.020(1)	0.5677(6)	0.250	5.0(2)
C5d	0.3294(8)	0.6817(4)	0.250	2.7(1)

complex corresponding to $[V_2(Hdpot)_2]^{2-}$ were not successful, a 2 : 1 vanadium(III)–tphpn complex (**2**) corresponding to **1** was obtained using benzoate as an additional bridging ligand. However, it has been revealed by X-ray crystallography that **2** has a bridging mode different from **1**, i.e., two vanadium(III) centers are bridged by an additional hydroxo bridge together with the alkoxo bridge of tphpn and the carboxylato bridge of bza, as in **1**.

Tables 4 and 5 summarize the final atomic parameters and the selected interatomic distances and angles of **2**, respectively. Figure 2 shows a perspective view of the complex cation with the numbering scheme. The complex cation has a symmetry plane, and the two equivalent vanadium(III) centers are linked by three different functional groups, that is, the alkoxo group of the tphpn, the carboxylato group of the bza, and the hydroxy group. As a consequence, each vanadium(III) center adopts a heptacoordinate structure, which differs from the hexacoordinate one found in **1b**. The coordination polyhedron of **2** can be described as a capped octahedron that is distinct from the pentagonal bipyramid of $[V_2(Hdpot)_2]^{2-}$, as discussed in a preliminary report.[3] The O1, O2, O1d, O1w, N1a, and N1b atoms form a distorted octahedron and the N1 atom occupies a capping position. A square base-trigonal cap polyhedron is an alternative description of the coordination polyhedron (see Ref. 3).

The coordination bond lengths in **2** are longer on average than those in **1b**, reflecting an increase of the coordination

Table 5. Selected Bond Distances (Å) and Angles (°) for $[V_2(bza)(OH)(tphpn)(H_2O)_2]Cl_3 \cdot 8H_2O$

Bond distances			
V–O1	2.022(3)	V–O2	2.023(3)
V–O1d	2.050(4)	V–O1w	2.108(4)
V–N1	2.241(5)	V–N1a	2.271(5)
V–N1b	2.191(5)	V···V′	3.228(1)
Bond angles			
O1–V–O2	71.7(2)	O1–V–O1d	86.9(2)
O1–V–N1	73.9(2)	O1–V–N1a	119.1(2)
O1–V–N1b	105.3(2)	O2–V–O1d	87.0(2)
O2–V–O1w	83.8(2)	O2–V–N1b	86.1(2)
O1d–V–O1w	82.7(2)	O1d–V–N1	123.5(2)
O1d–V–N1a	74.7(2)	O1d–V–N1b	163.3(2)
O1w–V–N1a	81.2(2)	O1w–V–N1b	81.4(2)
N1–V–N1a	70.2(2)	N1–V–N1b	71.8(2)
N1a–V–N1b	107.8(2)	V–O1–V′	105.9(2)
V–O2–V′	105.8(2)		

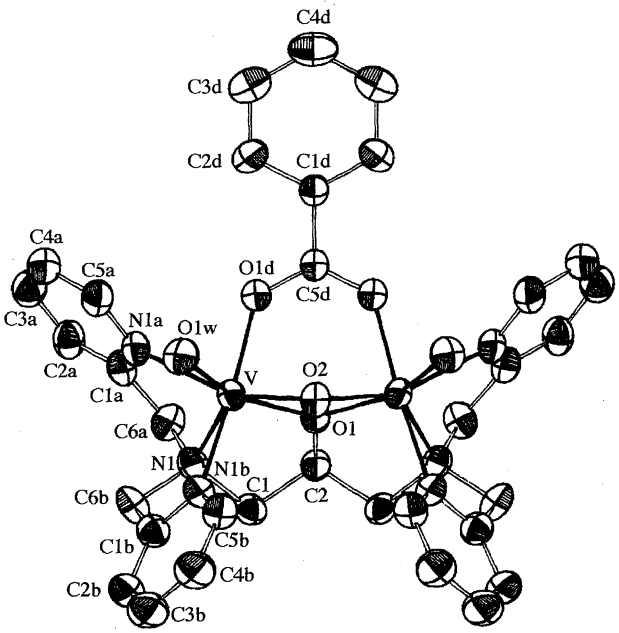

Fig. 2. Perspective view of $[V_2(bza)(OH)(tphpn)(H_2O)_2]^{3+}$ in **2**.

number. The alkoxo bridging angle, V–O1–V′ (105.9(2)°), is rather small compared to the corresponding one in **1b** (131.3(1)°). The additional hydroxo bridge would be responsible for the small bridging angle. The change in the alkoxo bridging angle also reflects in the V···V distance (3.228(1) Å), which in **2** is shorter than that in **1b** (3.593(2) Å), and in the V–O1d–C5d angle (130.8(4)°) is smaller than the corresponding one in **1b** (av. 137.7°). The V···V distance and V–O1d–C5d angle in **2** are comparable to the corresponding ones (3.250 Å and av. 129.8°) in a triply bridged dinuclear vanadium(III) complex, $[V_2L_2(\mu\text{-O})(\mu\text{-}CH_3COO)_2]^{2+}$ (L = 1,4,7-trimethyl-1,4,7-triazacyclononane).[7]

The $N(CH_2\text{-py})_2$ moiety of the tphpn in **2** coordinates to the vanadium center in a facial fashion, which is in contrast to a meridional coordination in the octahedral manganese complexes.[21–24]

In the diffuse reflectance spectrum of **2** in the 300—900 nm region, three bands were observed at 376, 539, and ca. 800 nm. Among these bands, the longest wavelength one is due to a transition diagnostic to heptacoordination of vanadium(III) complexes.[1,25] In addition to the above three bands, an aqueous solution of **2** exhibits a new band at 462 nm. It was found that the intensity of this band decreased with decreasing the pH of the solution. This observation suggests that the appearance of the 462-nm band in aqueous solution would be due to a deprotonation of the aqua ligand or the bridging hydroxo group of **2**. The protonation-deprotonation equilibrium of the bridging group has been reported for $[V^{III}_2L_2(\mu\text{-}O)(\mu\text{-}RCOO)_2]$ (L = 1,4,7-trimethyl-1,4,7-triazacyclononane[8] or hydridotripyrazolylborate.[9]

hpnbpda Complex. As shown above, the two alkoxo-bridging dinucleating ligands, dpot and tphpn, yield dinuclear vanadium(III) complexes with different structures. Since hpnbpda has an intermediate structure between dpot and tphpn, it is of interest to examine whether hpnbpda would act like dpot or tphpn. It was found that hpnbpda yields 2 : 2 complexes (**3a** and **3b**) corresponding to $[V_2(Hdpot)_2]^{2-}$, and a 2 : 1 complex (**4**) corresponding to $[V_2(dpot)(bza)(H_2O)_2]$. These facts indicate that hpnbpda acts in a manner similar to dpot, rather than tphpn, in constructing dinuclear vanadium(III) complexes. The observed difference in the coordination manner among the dinucleating ligands may be related to the different charge of the ligands. For example, a 2 : 2 complex with tphpn must have a high positive charge, +4, which would be unfavorable.[26]

$[V_2(hpnbpda)_2]$ crystallized into two different forms, orange form (**3a**) and yellow form (**3b**). The structure of **3a** was determined by X-ray crystallography. The final atomic coordinates and the selected bond lengths and angles are listed in Tables 6 and 7, respectively. Figure 3 depicts a perspective view of **3a** with the atom-numbering scheme. The X-ray analysis revealed that **3a** is a dinuclear vanadium(III) complex with two alkoxo bridges. The two vanadium(III) centers are equivalent, since the complex has a C_2-axis. The hpnbpda ligand acts as a heptadentate ligand. One 2-methylpyridyl group is free from coordination to the vanadium(III) center.[27] This selection seems to be reasonable, since a hard vanadium(III) atom would prefer a hard carboxylate oxygen atom to a soft pyridyl nitrogen atom.

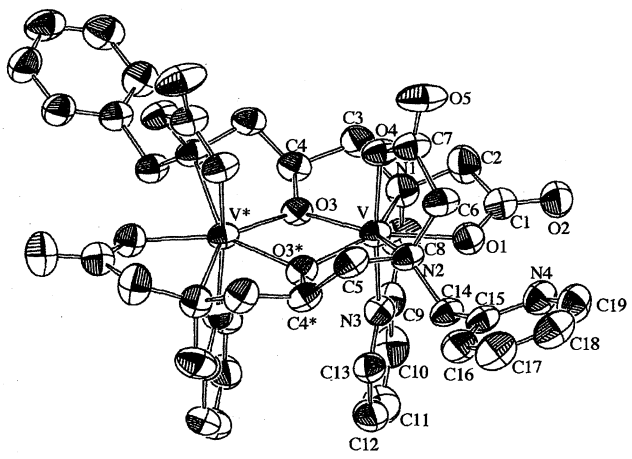

Fig. 3. Perspective view of $[V_2(hpnbpda)_2]$ (orange form) in **3a**.

Table 6. Final Atomic Coordinates and Equivalent Isotropic Thermal Parameters (B_{eq}/Å^2) for $[V_2(hpnbpda)_2]\cdot 12H_2O$ ($B_{eq}=(8\pi^2/3)\sum\sum U_{ij}a_i^*a_j^*\boldsymbol{a}_i\cdot\boldsymbol{a}_j$)

Atom	x	y	z	B_{eq}
V	−0.09074(5)	0.30874(5)	0.21651(4)	3.16(2)
O1	−0.2006(2)	0.3003(2)	0.1727(2)	4.01(8)
O2	−0.3276(2)	0.3223(3)	0.1819(2)	5.7(1)
O3	−0.0232(2)	0.2976(2)	0.3068(1)	3.31(7)
O4	−0.1010(2)	0.4399(2)	0.2270(2)	4.00(8)
O5	−0.1341(3)	0.5651(2)	0.1762(2)	6.3(1)
N1	−0.1706(2)	0.2890(3)	0.3066(2)	4.08(10)
N2	−0.0813(2)	0.3611(2)	0.1016(2)	3.38(9)
N3	−0.0974(2)	0.1709(2)	0.2167(2)	3.51(9)
N4	−0.2007(3)	0.3627(3)	−0.0397(2)	4.4(1)
C1	−0.2617(3)	0.3144(4)	0.2079(3)	4.4(1)
C2	−0.2472(3)	0.3265(4)	0.2865(3)	5.3(1)
C3	−0.1363(3)	0.3368(4)	0.3682(2)	4.3(1)
C4	−0.0509(3)	0.3131(3)	0.3757(2)	3.6(1)
C5	0.0018(3)	0.3840(3)	0.0926(2)	3.9(1)
C6	−0.1277(3)	0.4420(3)	0.1016(2)	4.0(1)
C7	−0.1199(3)	0.4867(3)	0.1734(3)	4.2(1)
C8	−0.1768(4)	0.1939(4)	0.3211(3)	5.4(1)
C9	−0.1384(3)	0.1359(3)	0.2695(3)	4.0(1)
C10	−0.1439(3)	0.0461(4)	0.2764(3)	5.2(1)
C11	−0.1076(4)	−0.0071(4)	0.2288(4)	5.9(2)
C12	−0.0671(3)	0.0290(4)	0.1746(3)	5.0(1)
C13	−0.0627(3)	0.1180(3)	0.1704(3)	4.0(1)
C14	−0.1103(3)	0.2988(3)	0.0450(2)	3.7(1)
C15	−0.1265(3)	0.3382(3)	−0.0273(2)	3.7(1)
C16	−0.0706(3)	0.3472(4)	−0.0770(3)	4.7(1)
C17	−0.0907(4)	0.3840(4)	−0.1425(3)	5.5(2)
C18	−0.1658(4)	0.4091(4)	−0.1556(3)	5.5(2)
C19	−0.2183(4)	0.3971(4)	−0.1036(3)	5.4(1)

Table 7. Selected Bond Distances (Å) and Angles (°) for $[V_2(hpnbpda)_2]\cdot 12H_2O$

Bond distances			
V–O1	2.044(3)	V–O3	2.038(3)
V–O3*	2.029(3)	V–O4	2.037(3)
V–N1	2.235(4)	V–N2	2.320(4)
V–N3	2.125(4)	V···V*	3.334(2)
Bond angles			
O1–V–O4	91.2(1)	O1–V–N1	73.4(1)
O1–V–N2	74.7(1)	O1–V–N3	83.6(2)
O3–V–O3*	69.1(1)	O3–V–O4	93.0(1)
O3–V–N1	72.8(1)	O3–V–N3	86.8(1)
O3*–V–O4	101.1(1)	O3*–V–N2	74.5(1)
O3*–V–N3	88.2(1)	O4–V–N1	90.3(2)
O4–V–N2	75.8(1)	O4–V–N3	170.0(2)
N1–V–N3	80.1(2)	N2–V–N3	110.7(1)
V–O3–V*	110.1(1)		

Each vanadium(III) center of **3a** is situated in a distorted pentagonal-bipyramidal structure. O1, N2, O3*, O3, and N1 atoms complete the pentagonal plane, and O4 and N3 atoms

occupy the axial positions. The sum of the in-plane angles is 364.5°, deviating by only 4.5° from 360°. The largest deviations from the least-squares plane (O1, O3, O3*, N1, N2) are found for N1 (−0.369(5) Å) and N2 (0.732(4) Å). The trans angle, defined by the O4, V, and N3 atoms, is 170.0(2)° near to 180°. Thus, the coordination polyhedron adopted by the vanadium(III) center in **3a** can be reasonably ascribed to a pentagonal bipyramid.

The bond distances and angles in **3a** are comparable to those in $[V_2(Hdpot)_2]^{2-}$.[1] The V···V* separation is 3.334(2) Å, which is shorter than that in **1b**, but larger than in **2**. Intramolecular stacking is recognized between the two coordinated pyridyl groups (ca. 3.67 Å).

Figure 4 compares the diffuse reflectance spectrum of **3a** with the absorption spectrum in methanol. The absorption spectrum corresponds well to the reflectance spectrum, indicating that the structure found in the crystals is maintained in methanol. The broad band around 800 nm is of typical to heptacoordinate vanadium(III) complexes, as mentioned in the above section.[1,25]

We could not obtain crystals of the yellow form (**3b**) suitable for single-crystal X-ray analysis. The structure of **3b** was, therefore, estimated based on its spectroscopic properties. Figure 5 shows the diffuse reflectance and absorption spectra of **3b**. The broad band around 800 nm suggests that **3b** also has a heptacoordinate structure. In addition to this band, the band at 370 nm was observed both in **3a** and **3b**, but the 522 nm band of **3a** shifts to 490 nm in **3b**. This shift would indicate that some change in the arrangement of the coordinating atoms may occur in **3b**. A possibility of **3b** to be a monomeric complex can be completely neglected on the basis of the magnetic properties of **3b** discussed in the following section. One possible structural change would be a replacement of the coordinated carboxylate group with the free pyridyl group in **3a**. However, a crucial difference was not found in the carboxylate stretching region of the infrared

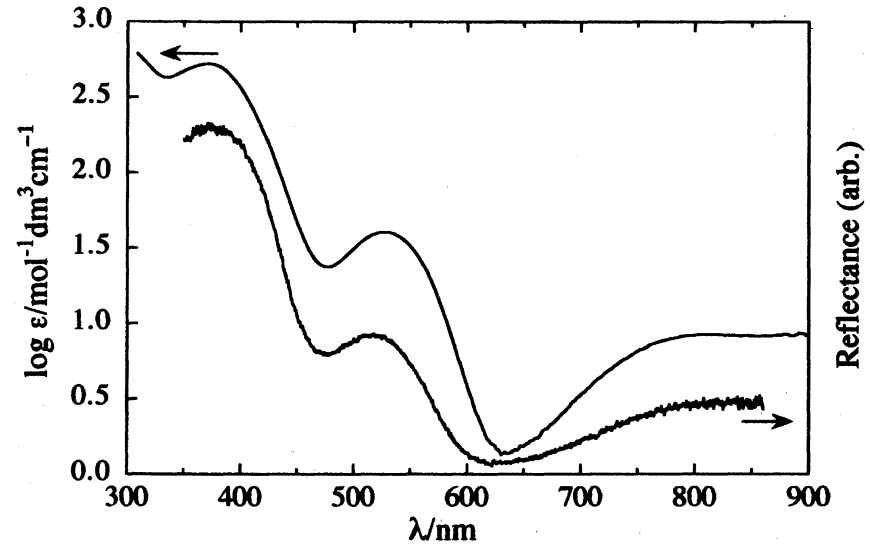

Fig. 4. Absorption (in methanol) and diffuse reflectance spectra of **3a**.

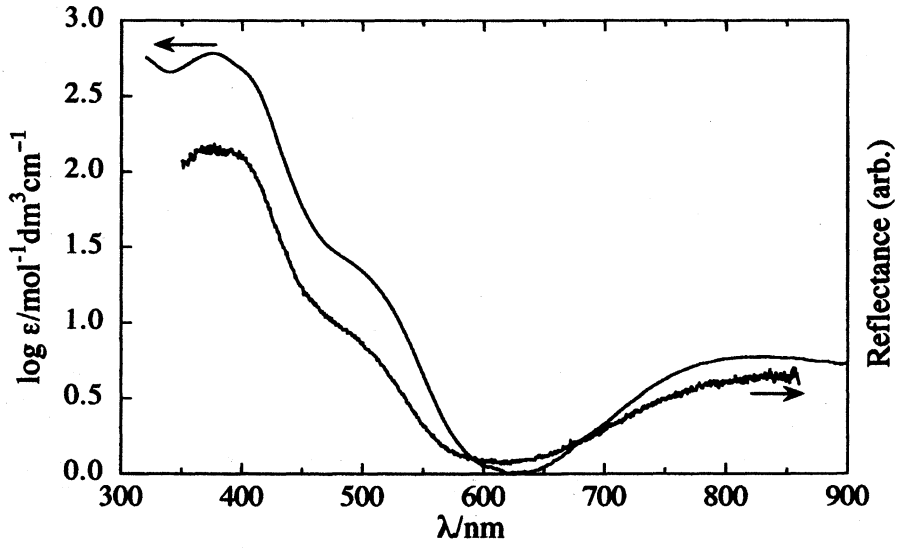

Fig. 5. Absorption (in methanol) and diffuse reflectance spectra of **3b**.

spectra between **3a** and **3b**. Thus, a release of the carboxylate group from the coordination site is not likely. Another possible structural change would be an interchange of the positions between the coordinating carboxylate group and the coordinating pyridyl group of the $N(CH_2COO^-)(CH_2\text{-py})$ moiety in **3a**. This interchange of the coordinating positions would be most likely to occur.

The absorption spectrum of **3a** in methanol changed very slowly to that of **3b**, indicating that **3a** slowly isomerizes to **3b**. The absorption spectrum of **3b** in methanol did not change at all. These observations suggest that **3b** is a more stable form than **3a**.

Although the elemental analysis and the infrared spectrum suggest that **4** has a structure similar to **1a**, further characterization was not done because of its instability.

Magnetic Properties. Dinuclear vanadium(III) complexes show a variety of intramolecular spin-exchange coupling depending on the bridging mode. It is, therefore, of interest to examine the spin-exchange coupling of the dinuclear vanadium(III) complexes obtained here. Figures 6 and 7 show the magnetic susceptibility (χ_a/V) and the effective magnetic moment (μ_{eff}/V) of **1a** and **2**, respectively, as a function of the temperature in region of 2 to 300 K. The effective magnetic moment (μ_{eff}) of **1a** increases from 2.86 μ_B at 300 K with decreasing temperature, and reaches 3.36 μ_B around 10 K. For **2** μ_{eff} varies from 2.78 μ_B at 300 K to 3.46 μ_B around 10 K. The values at 300 K are comparable to the value expected for a magnetically isolated V^{III} (d^2) ion (2.83 μ_B). The above observations indicate a ferromagnetic coupling for **1a** and **2**. The temperature dependence of the magnetic susceptibility for **1a** and **2** was analyzed on the basis of the spin-Hamiltonian $H=-2JS_1\cdot S_2$ ($S_1=S_2=1$). The temperature-independent paramagnetism (T. I. P.) was neglected in the calculation. A least-squares fit to the experimental data, shown as a solid line in Figs. 6 and 7, yielded $J=23.7$ cm^{-1} and $g=1.90$ for **1a** and $J=14.6$ cm^{-1} and

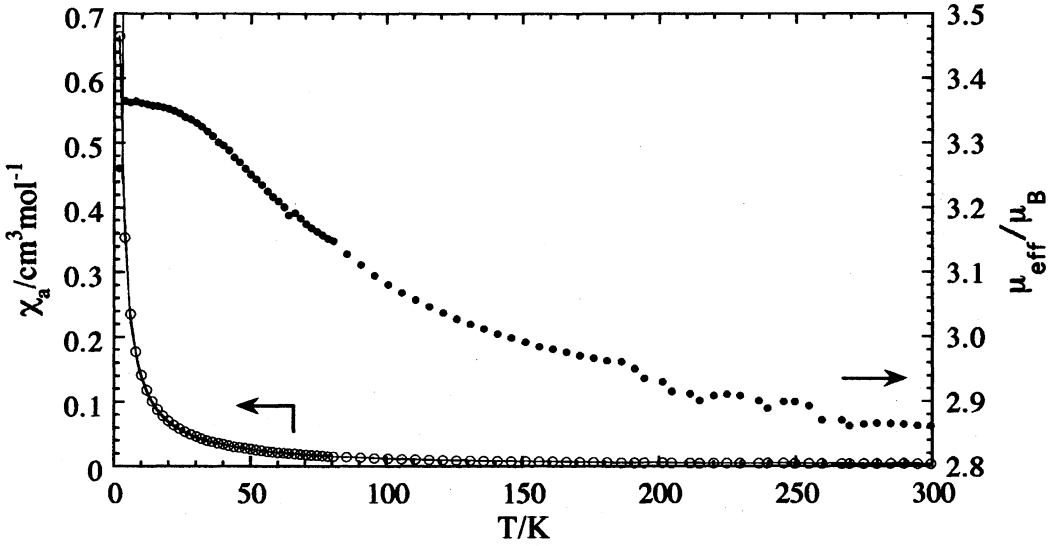

Fig. 6. Plot of the magnetic susceptibility and the effective magnetic moment against temperature for **1a**.

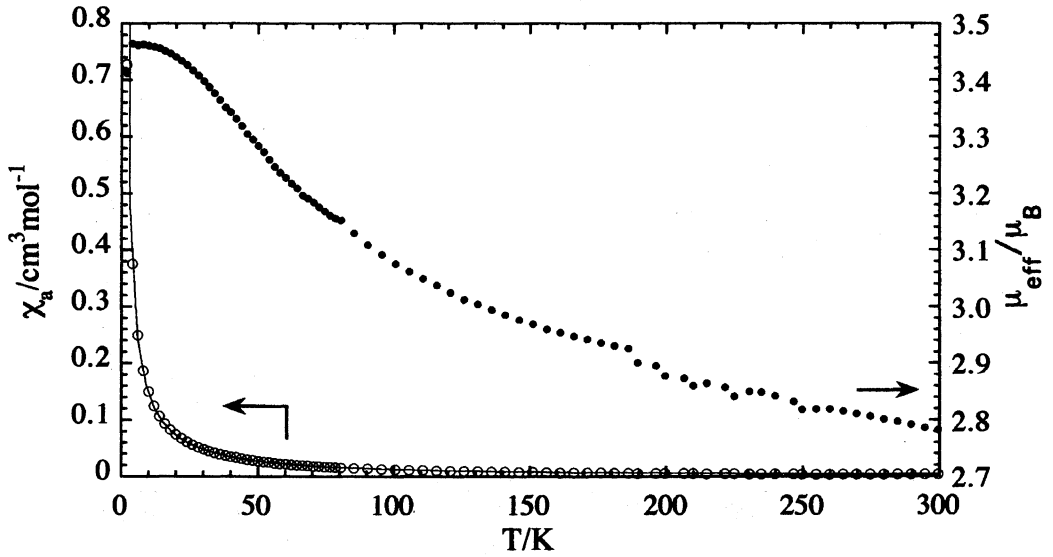

Fig. 7. Plot of the magnetic susceptibility and the effective magnetic moment against temperature for **2**.

$g = 1.98$ for **2**.

It is noteworthy that **1a** and **2** are the first examples of dinuclear vanadium(III) complexes exhibiting a ferromagnetic exchange coupling without an oxo bridge; all of the earlier examples that exhibit a ferromagnetic coupling contain an oxo bridge.[4–9] Another noticeable point is that **1a** and **2** show a similar magnetic behavior, despite the fact that **2** has a hydroxo bridge in addition to the alkoxo and carboxylato bridges, as in **1a**; as a result, **2** adopts a heptacoordinate structure, whereas **1a** adopts a hexacoordinate structure.

In contrast to **1a** and **2**, **3a** and **3b** exhibit an antiferromagnetic spin-exchange coupling similar to the structurally related $[V_2(Hdpot)_2]^{2-}$ complex,[1] as shown in Figs. 8 and 9, respectively. The effective magnetic moment for **3a** and **3b** decreases from 2.44 μ_B at 300 K and approaches to 0 μ_B with decreasing temperature. The magnetic susceptibility increases with decreasing temperature and reaches a maximum at ca. 100 K for **3a** and ca. 72 K for **3b**. Then, χ_a decreases with decreasing temperature. This behavior is typical of an antiferromagnetically coupled dinuclear species. The solid lines in Figs. 8 and 9 represent the fit of the experimental data to the same model as that employed for **1a** and **2**. The best-fit parameters are $J = -35.2$ cm^{-1} and $g = 1.98$ for **3a**, and $J = -25.4$ cm^{-1} and $g = 1.88$ for **3b**. These J values indicate a larger antiferromagnetic interaction compared to other dinuclear vanadium(III) complexes containing two alkoxo bridges, $[V_2(Hdpot)_2]^{2-}$ (-14.5 cm^{-1})[1] and $[V_2(hedtaH)_2]^{2-}$ (-8.6 cm^{-1}).[10]

Electrochemistry. The redox behavior of **3a** has been examined by cyclic voltammetry in a methanol solution containing 0.1 mol dm^{-3} tetra-*n*-butylammonium perchlorate as supporting electrolyte at a glassy carbon working electrode and a Ag/AgCl reference electrode; the result is shown in Fig. 10. **3a** exhibits one reversible one-electron-transfer wave at +0.65 V vs. Ag/AgCl ($\Delta E_p = E_{p,red} - E_{p,ox} = 70$ mV) and a quasi-reversible one-electron-transfer wave at +1.02

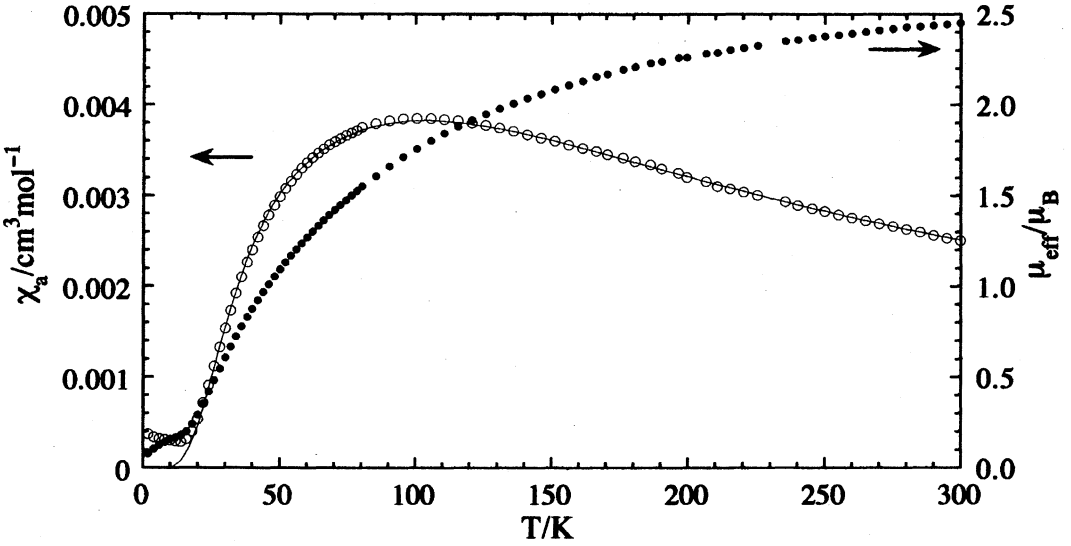

Fig. 8. Plot of the magnetic susceptibility and the effective magnetic moment against temperature for **3a**.

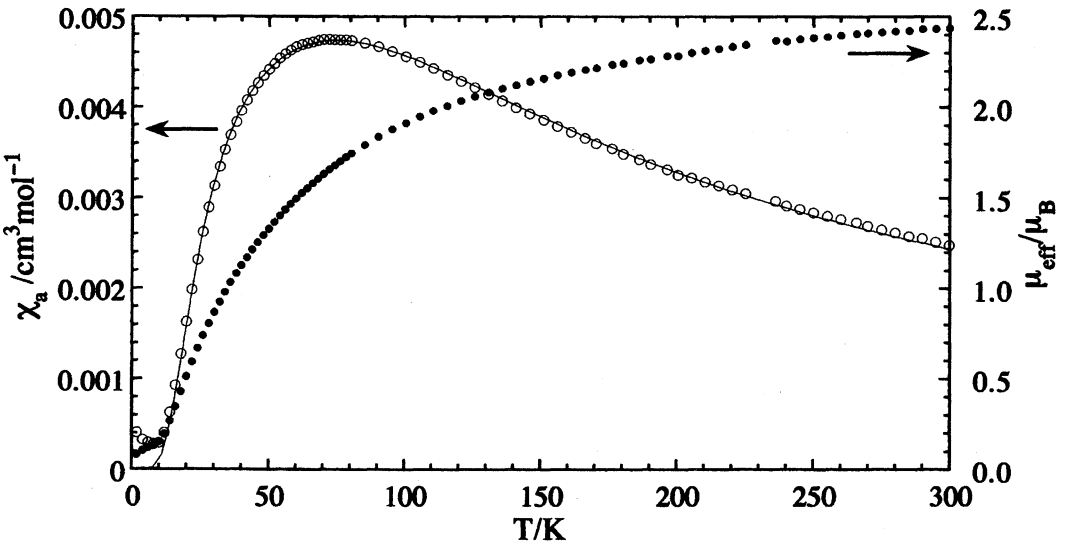

Fig. 9. Plot of the magnetic susceptibility and the effective magnetic moment against temperature for **3b**.

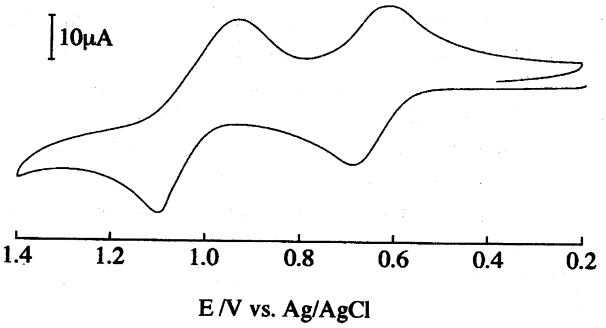

Fig. 10. Cyclic voltammogram of **3a** in methanol; scan rate 200 mV s^{-1}.

V vs. Ag/AgCl ($\Delta E_p = 170$ mV), which correspond to the couples $V^{IV}V^{III}/V^{III}V^{III}$ and $V^{IV}V^{IV}/V^{IV}V^{III}$, respectively. At slow scan rates (20 mV s^{-1}), although the first redox process still remains reversible, the second process becomes irreversible, indicating the instability of the $V^{IV}V^{IV}$ form of **3a** in solution.

In contrast to **3a**, **3b** displays two irreversible oxidation waves at +0.81 and +1.22 V vs. Ag/AgCl under the experimental conditions, where **3b** exhibits two reversible redox processes, indicating the very low stability of the oxidized form of **3b**. Similarly, **1** exhibits two irreversible oxidation waves at +0.96 and +1.32 V vs. Ag/AgCl. An electrochemical study was not undertaken for **2**, because of its low solubility.

This work was partially supported by a Grant-in-Aid for Scientific Research from the Ministry of Education, Science, Sports and Culture.

References

1) a) J. C. Robles, M. Shimoi, and H. Ogino, *Chem. Lett.*, **1992**, 309; b) J. C. Robles, Y. Matsuzaka, S. Inomata, M. Shimoi, W. Mori, and H. Ogino, *Inorg. Chem.*, **32**, 13 (1993).

2) K. Kanamori, K. Yamamoto, and K. Okamoto, *Chem. Lett.*, **1993**, 1253.

3) K. Kanamori, T. Okayasu, and K. Okamoto, *Chem. Lett.*, **1995**, 105.

4) P. Knopp, K. Wieghardt, B. Nuber, J. Weiss, and W. S. Sheldrick, *Inorg. Chem.*, **29**, 363 (1990).

5) S. G. Brand, N. Edelstein, C. J. Hawkins, G. Shalimoff, M. R. Snow, and E. R. T. Tiekink, *Inorg. Chem.*, **29**, 434 (1990).

6) K. Kanamori, E. Kameda, T. Kabetani, T. Suemoto, K. Okamoto, and S. Kaizaki, *Bull. Chem. Soc. Jpn.*, **68**, 2581 (1995).

7) M. Köppen, G. Fresen, K. Wieghardt, R. M. Llusar, B. Nuber, and J. Weiss, *Inorg. Chem.*, **27**, 721 (1988).

8) P. Knopp and K. Wieghardt, *Inorg. Chem.*, **30**, 4061 (1991).

9) C. J. Carrano, R. Verastgue, and M. R. Bond, *Inorg. Chem.*, **32**, 3589 (1993).

10) R. E. Shepherd, W. E. Hatfield, D. Ghosh, C. D. Stout, F. J. Kristine, and J. R. Ruble, *J. Am. Chem. Soc.*, **103**, 5511 (1981).

11) S. Lee, K. Nakanishi, M. Y. Chiang, R. B. Frankel, and K. Spartalian, *J. Chem. Soc., Chem. Commun.*, **1988**, 785.

12) R. J. Bouma, J. H. Teuben, W. R. Beukema, R. L. Bansemer, J. C. Huffmann, and K. G. Caulton, *Inorg. Chem.*, **23**, 2715 (1984).

13) D. J. Hodgson, *Prog. Inorg. Chem.*, **19**, 173 (1975).

14) J. R. Rambo, S. L. Bartley, W. E. Streib, and G. Christou, *J. Chem. Soc., Dalton Trans.*, **1994**, 1813.

15) N. S. Dean, S. L. Bartley, W. E. Streib, E. B. Labkovsky, and G. Christou, *Inorg. Chem.*, **34**, 1608 (1995).

16) M. Suzuki, T. Sugisawa, H. Senda, H. Oshio, and A. Uehara, *Chem. Lett.*, **1989**, 1091.

17) M. K. Chan and W. H. Armstrong, *J. Am. Chem. Soc.*, **111**, 9121 (1989).

18) "Enraf–Nonius Structure Determination Package (SDP)," Enraf–Nonius, Delft, The Netherlands (1978).

19) C. K. Fair, "MOLEN, International Structure Solution Procedure," Enraf–Nonius, Delft, The Netherlands (1990).

20) Molecular Structure Corporation, "teXsan. Single Crystal Structure Analysis Software. Version 1.7. MSC, 3200 Research Forest Drive," The Woodlands, TX 77381, USA (1995).

21) M. K. Chan and W. H. Armstrong, *J. Am. Chem. Soc.*, **111**, 9121 (1989).

22) M. Suzuki, T. Sugisawa, H. Senda, H. Oshio, and A. Uehara, *Chem. Lett.*, **1989**, 1091.

23) M. K. Chan and W. H. Armstrong, *J. Am. Chem. Soc.*, **112**, 4985 (1990).

24) M. L. Kirk, M. K. Chan, W. H. Armstrong, and E. I. Solomon, *J. Am. Chem. Soc.*, **114**, 10432 (1992).

25) K. Kanamori, K. Ino, H. Maeda, K. Miyazaki, M. Fukagawa, J. Kumada, T. Eguchi, and K. Okamoto, *Inorg. Chem.*, **33**, 5547 (1994).

26) This account was based on the kind suggestion by one of the referees.

27) The position of the nitrogen atom in the free pyridyl group was determined based on the bond distances (see Supplemental Materials).